J. Fluid Mech. (1976), *vol.* 76, *part* 4, *pp.* 675–688
Printed in Great Britain

Shock attenuation by a single transverse slit

By J. H. S. LEE, P. P. OSTROWSKI† AND J. H. T. WU
Department of Mechanical Engineering, McGill University, Montreal, Canada

(Received 12 September 1975 and in revised form 27 April 1976)

Attenuation of a plane shock due to the interaction with a single slit is examined via spark schlieren photography for shock Mach numbers between 1·17 and 2·44 and slit widths between 0·173 and 3·175 cm. Wave speed measurements by piezoelectric transducers indicate that the attenuation is weak and adequately predicted by Whitham's ray-shock theory. The slit width is observed to produce only a secondary effect on the shock attenuation rate. Stability of the attenuating shock is demonstrated from a wave diagram constructed by the ray-shock technique.

1. Introduction

Recently there has been a revival of interest in the interaction of travelling shock waves with various obstacles owing to the growing concern regarding unconfined vapour cloud explosions associated with the storage and transport of large quantities of petrochemicals. Investigation of the gasdynamic aspects of such explosions‡ can provide valuable information concerning the design of blast-resistant structures and the placement of storage and processing facilities relative to population centres. In addition, there appears to be a real need for investigation into practical methods of dissipating and attenuating shock waves which may be generated by other types of industrial accidents.

The present study examines the attenuation of an initially planar shock wave as it passes over a single slit in the wall of a rectangular duct of constant cross-section. Attenuation results from diffraction of the shock through the slit and the generation of a transversely propagating expansion fan which interacts with the shock and weakens it. This process is offset somewhat by the subsequent reflexion of the diffracted shock from the downstream edge of the slit, which then gives rise to a transversely propagating shock wave as well. Both transverse waves undergo multiple reflexions from the walls as the main shock proceeds down the duct. After some period of time, a steady fluid jet will be established at the slit. A sketch illustrating the wave configurations for several successive shock positions is presented in figure 1.

Intuitively, the attenuation process must be both weak and gradual since the

† Present address: Department of Mechanical Engineering, University of Maryland, College Park, Md.

‡ Investigation into the hazards connected with storage and transport of LNG, Working Program 1974, Technologisch Laboratorium, Rijswijk, Netherlands, 1974.

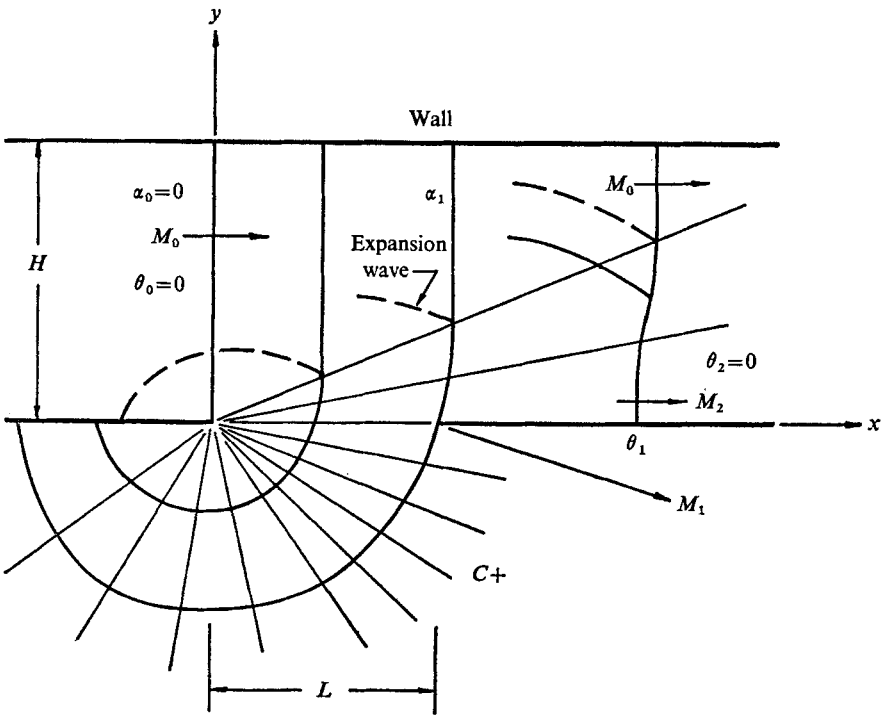

FIGURE 1. Wave configurations for shock attenuation in a rectangular channel with a slit in one wall. L = slit width.

energy loss through the slit is communicated to the shock via transverse waves which not only tend to compensate each other but also require a finite time to traverse the shock. Owing to the multiple reflexions of the transverse waves, it is evident that the duct wall spacing governs the rate at which the attenuation process proceeds. Spreading of the transverse waves reduces their effectiveness, so that subsequent disturbances in the flow field which reach the shock via re-reflected waves are then likely to be weak. Thus the wave speed along either wall follows a cyclic variation, the amplitude of which must gradually decrease.

Under all but the most extreme conditions, the reflexion process at the downstream edge of the slit will be a non-stationary Mach reflexion. Since this, as well as the initial diffraction of the shock through the slit, is easily handled by Whitham's (1957) ray-shock theory, that method is adopted for the theoretical analysis. The ray-shock technique will also be employed for the construction of a wave diagram which describes the motion of the transverse waves on the shock front. This is used to illustrate the cyclic variations in shock Mach number as well as the stability of the attenuating shock.

2. Theory

In accordance with the ray-shock theory, an orthogonal curvilinear co-ordinate system (α, β) is chosen, where α represents the instantaneous shock shape at time t and β gives the orthogonal trajectories (rays) of arbitrary points on the shock front. By considering the rays to be equivalent to solid boundaries Whitham (1958) applied the well-known CCW relation, describing the motion of a shock wave in a channel, to the ray tubes. From this relation and the geometry of the co-ordinate system it was demonstrated that the shock shape can be determined for all times by the method of characteristics.

For the present problem, only the internal flow will be considered in detail. Since most of the shock diffraction occurs outside the slit, inside the shock Mach number variations are small, hence the slowly varying Chester function $K(M)$ employed in Whitham's analysis may be treated as a constant at some suitable average value. This approximation considerably simplifies the mathematical analysis (Oshima *et al.* 1965).

According to the ray-shock theory, the diffraction process at the upstream edge of the slit corresponds to the formation of a simple wave, so that the positive $(C+)$ characteristics are straight and centred at the origin (figure 1). Furthermore, Whitham deduced that in this case the Mach number M and inclination of the rays θ are constant along each $C+$. The latter is given by (Whitham 1958; Oshima *et al.* 1965)

$$\theta(M) = \ln\left[\frac{M+(M^2-1)^{\frac{1}{2}}}{M_0+(M_0^2-1)^{\frac{1}{2}}}\right]^{n^{\frac{1}{2}}} = n^{\frac{1}{2}}(\cosh^{-1}M - \cosh^{-1}M_0), \tag{1}$$

where M_0 is the undisturbed shock Mach number, $\theta_0 = 0$ and $n = 2/K(M)$ may be taken to be that computed from the average of M and M_0. The local shock Mach number M_1 approaching the downstream edge of the slit may then be determined by integration along the $C+$ characteristic which coincides with the x axis.

The characteristic co-ordinates for the general case are illustrated in figure 2. Here, α and β are chosen in the usual way so that the co-ordinate distances are as shown. The angle m between a $C+$ and a ray is given by (Whitham 1958; Skews 1972)

$$\tan m = \frac{Ad\beta}{Md\alpha} = \frac{1}{M}\left(\frac{M^2-1}{n}\right)^{\frac{1}{2}}, \tag{2}$$

where A is the ray-tube area. Then, according to figures 1 and 2 the shock co-ordinates (x_s, y_s) at any time t prior to reflexion are found by direct integration along a $C+$. These are (Skews 1972)

$$x_s = M\frac{\cos(\theta+m)}{\cos m}\alpha, \quad y_s = \frac{M\sin(\theta+m)}{\cos m}\alpha, \tag{3}$$

where $\alpha = c_0 t$ and c_0 is the (constant) sound speed ahead of the propagating shock.

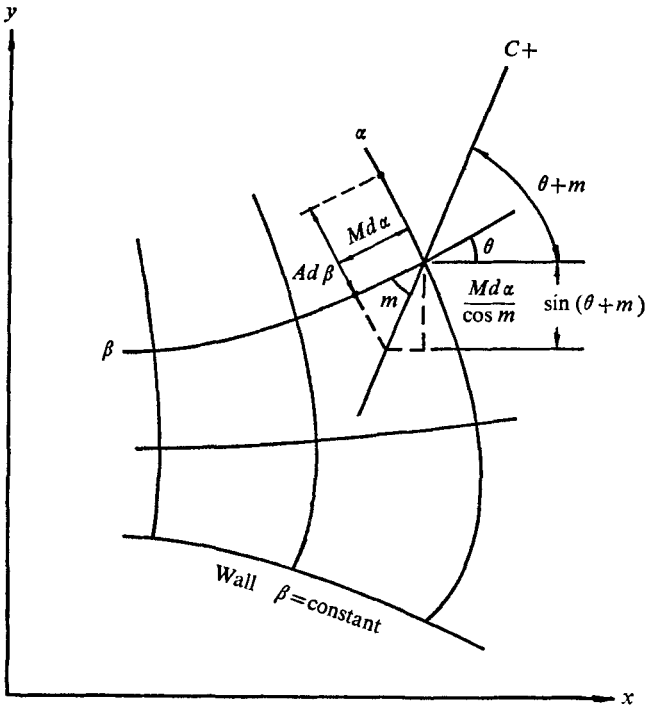

FIGURE 2. Characteristic co-ordinates in the x, y plane.

The shock Mach number M_1 which approaches the downstream edge of the slit at time α_1 is determined by setting $y_s = 0$ in (3), which yields

$$\theta_1 = -m(M_1). \tag{4}$$

Then making use of (1) and (2) gives

$$\left[\frac{(n_1+1)M_1^2-1}{n_1}\right]^{\frac{1}{2}} \cos\left[n_0^{\frac{1}{2}} \ln \frac{M_1+(M_1^2-1)^{\frac{1}{2}}}{M_0+(M_0^2-1)^{\frac{1}{2}}}\right] - M_1 = 0, \tag{5}$$

which is easily solved for M_1 by iteration. Here, $n_1 = 2/K(M_1)$ and n_0 is computed from the average of M_0 and M_1. Once M_1 is determined, θ_1 can be calculated from (1). More generally, the shape of the diffracted shock may be determined by a similar approach.

Analysis of the Mach reflexion process at the downstream edge of the slit is relatively simple if it is assumed that both the incident shock and resulting Mach stem are straight. Since most of the diffraction occurs outside the slit, the induced curvature may be small enough to be disregarded locally as a first approximation. With this in mind, an idealized representation of the reflexion process at the downstream edge of the slit is presented in figure 3. The incident shock Mach number is M_1, the deflexion angle is θ_1 and the attenuated shock Mach number (the Mach stem) is M_2.

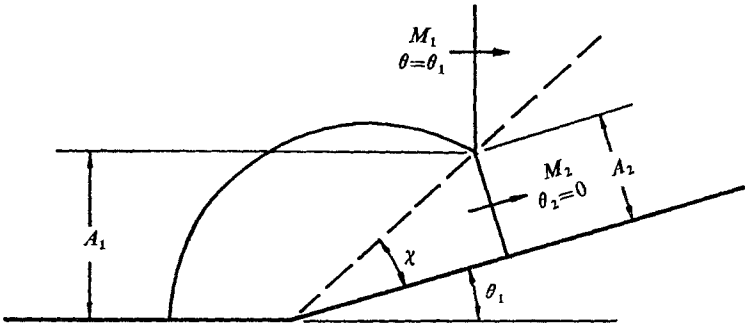

FIGURE 3. Idealized representation of the Mach reflexion process at the downstream edge of the slit.

The situation shown in figure 3 has been described by Whitham (1958), who found that

$$\tan\theta_2 = \frac{\{(M_2^2-M_1^2)[1-(A_2/A_1)^2]\}^{\frac{1}{2}}}{M_1+M_2(A_2/A_1)}. \tag{6}$$

The area ratio A_2/A_1 is given by the integrated form of the CCW relation

$$\frac{A_2}{A_1} = \left[\frac{M_1^2-1}{M_2^2-1}\right]^{\frac{1}{2}n_2}, \tag{7}$$

where n_2 is now computed from the average of M_1 and M_2. Then, since

$$\theta_2 = -\theta_1 = m(M_1),$$

substitution of (2) and (7) into (6) yields

$$(M_2^2-M_1^2)\left[1-\left(\frac{M_1^2-1}{M_2^2-1}\right)^{n_2}\right] - \frac{M_1^2-1}{n_1}\left[1+\frac{M_2}{M_1}\left(\frac{M_1^2-1}{M_2^2-1}\right)^{\frac{1}{2}n_2}\right]^2 = 0, \tag{8}$$

which is again easily solved for M_2 by iteration.

Experimental evidence indicates that the attenuation process described above is relatively weak; M_2 differs from M_0 by only a few per cent. Thus a fairly precise description of the diffraction and reflexion processes is required for an accurate solution of the problem. Unfortunately, the above solution does not lead to acceptable results and the difficulty can be attributed to the inherent inaccuracies of the ray-shock theory.

It was recognized by Whitham and later demonstrated by Skews (1972) that for the diffraction of low to moderate strength shocks the ray-shock theory does not accurately predict the angle m_0 associated with the head characteristic. From acoustic theory, the correct value was shown to be given by (Skews 1972)

$$\tan^2 m_0 = \frac{(M_0^2-1)[2+(\gamma-1)M_0^2]}{(\gamma+1)M_0^4}. \tag{9}$$

Now, if (9) is applied locally in place of (2), the modified form of (5) is then

$$\left(\frac{2\gamma M_1^4+(3-\gamma)M_1^2-2}{\gamma+1}\right)^{\frac{1}{2}} \cos\left[n_0^{\frac{1}{2}}\ln\frac{M_1+(M_1^2-1)^{\frac{1}{2}}}{M_0+(M_0^2-1)^{\frac{1}{2}}}\right] - M_1^2 = 0. \tag{10}$$

Equations (8) and (10) give the solution for the attenuated shock Mach number M_2 just downstream of the slit. It should be recognized, however, that the condition $\theta_1 = -m(M_1)$ is applied to (8) but not to (10) and the proposed solution is not really the correct one. It will be shown later that, in spite of this anomaly, reasonably good agreement with experiment is observed.

The above solution is the appropriate one only for an infinitely wide channel. For finite channel widths, multiple reflexions of the transverse waves from the walls result in further attenuation as the shock advances down the duct. This aspect of the attenuation process is most conveniently described by construction of a wave diagram.

According to the ray-shock theory the characteristics represent the trace of kinematic waves on the shock and the 'shock-shock' represents the path of the triple point of Mach reflexion, which is a discontinuity in the physical and characteristic planes. For the present problem four types of interaction must be considered. These are (i) characteristic intersections, (ii) characteristic reflexion from a solid boundary, (iii) crossing of a shock-shock by a characteristic, and (iv) shock-shock reflexion from a solid boundary. The first two cases are easily handled in the usual way by making use of the characteristic invariants (Whitham 1958),

$$C+ : P = \theta(M) + \omega(M) = \text{constant},$$
$$C- : Q = \theta(M) - \omega(M) = \text{constant},$$

where $\omega(M) = \ln[(M + (M^2-1)^{\frac{1}{2}})/(M_0 + (M_0^2-1)^{\frac{1}{2}})]^{n^{\frac{1}{2}}}$.

Interactions involving shock-shocks are more complicated as the characteristic invariants change discontinuously across them; θ and M are unknown after the interaction. The Mach reflexion equations provide one relation between M and θ although another is needed to complete the solution. Milton (1971) has suggested the following scheme. For a finite characteristic mesh, the curved Mach stem associated with the shock-shock is represented by a series of straight segments joined together. The point of connexion appropriate to two neighbouring characteristics which cross the shock-shock then follows some path (called a contiguity line) in the flow field. Since it is the characteristics which carry disturbances to the shock, the essence of Milton's method is to assume that the slope of the contiguity line is the average of the slopes of the two neighbouring characteristics. Denoting quantities downstream of a shock-shock by primes, the contiguity direction ψ corresponding to two neighbouring characteristics 1′ and 2′ is

$$\psi = \tfrac{1}{2}[(\theta_1' \pm m_1') + (\theta_2' \pm m_2')],$$

where the plus and minus signs are appropriate to the $C+$ and $C-$ characteristics respectively.

Then equating the components of the two Mach stem velocities in this direction gives

$$\frac{M_1' \, d\alpha}{\cos(\psi - \theta_1')} = \frac{M_2' \, d\alpha}{\cos(\psi - \theta_2')};$$

hence

$$\frac{M_2'}{M_1'} = \frac{\cos\tfrac{1}{2}(\theta_1' - \theta_2' \pm m_1' \pm m_2')}{\cos\tfrac{1}{2}(\theta_2' - \theta_1' \pm m_1' \pm m_2')}. \tag{11}$$

M_2' and θ_2' are then determined from (6) and (11) by iteration.

Shock-shock reflexion from a solid boundary is easily determined since the Mach stem must be normal to the wall after reflexion; i.e. $\theta_2 = 0$. Then $\Delta\theta$ for the reflexion process is just θ', which is the Mach stem orientation just prior to reflexion. The incident shock Mach number for the reflexion shock-shock becomes M_2'. The new stem shock Mach number is quickly determined from the Mach reflexion relations, equation (8).

Using the techniques described above, the wave diagram is then constructed step by step starting with the simple wave which corresponds to the initial shock diffraction process.

3. Experiments

A simple air/air shock tube with a square cross-section 5·23 cm by 5·23 cm was employed for all tests. This was constructed from structural steel tubing and consisted of 1·52 m driver and driven sections followed by a test section. Mylar sheet plastic was used as the diaphragm material.

Two separate test sections were employed. The first was constructed by milling away two opposite walls of a 12·70 cm segment of the tube and fitting glass plates in place with rubber gaskets for schlieren viewing. A 0·699 cm slit with a 30° chamfer was then milled into one of the remaining walls. Since it was necessary to perform the higher shock Mach number tests with an evacuated driven section, a second test section was built with an enclosure surrounding the slit. In this case removable flanges were fitted so that the slit width could be varied. A 10° external slit chamfer and ordinary plate-glass side walls were used in conjunction with this test section.

Photographic studies were carried out using a time-delayed spark schlieren optical system triggered by a pressure transducer located just upstream of the slit. With this test arrangement only one photograph could be obtained for each firing of the shock tube, so that the sequence of events near the slit was pieced together from the results of several separate runs. Reproducibility of the test conditions, which is crucial to the successful application of this technique, was observed to be satisfactory.

Additional data in the form of shock velocity measurements were obtained from two piezoelectric pressure transducers spaced 10·2 cm apart, with the first located 50 cm downstream of the slit. These were connected to the input terminals of a dual-beam oscilloscope (Tektronix Model 555) which was triggered by a third transducer.

4. Results and discussion

A sequence of 9 schlieren photographs depicting the shock–slit interaction for $M_0 = 1{\cdot}4$ and $L = 0{\cdot}699$ cm is presented in figure 4. Numbers on the left side of the photos give the time delay in microseconds relative to the instant the shock passes the spark–lamp–trigger–transducer, 7·30 cm ahead of the slit. The field of view is roughly 4·5 cm by 8·3 cm.

Figures 4(*a*) and (*b*) (plate 1) depict the shock diffraction through the slit and

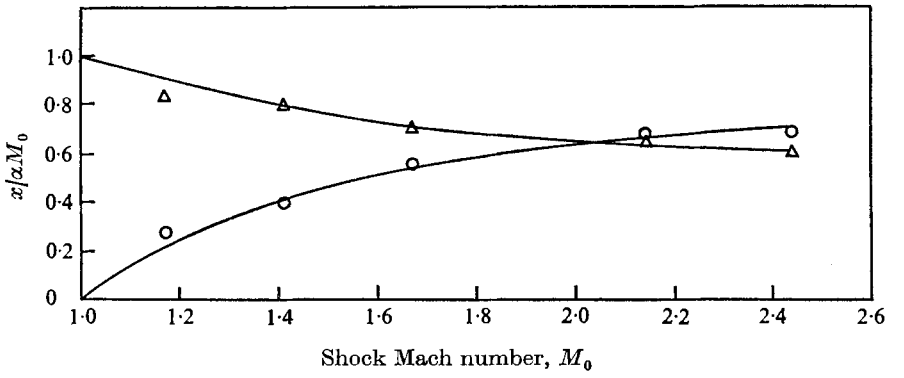

FIGURE 6. ○, expansion wave centre, $x_e = u_1 t$; △, expansion wave radius, $r_e = c_1 t$.

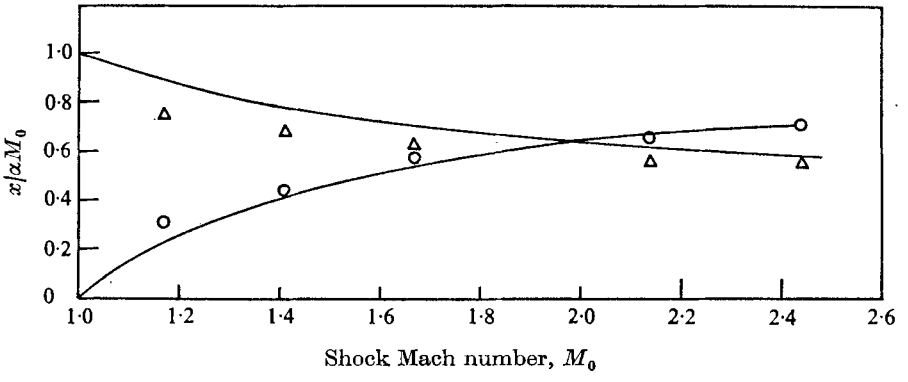

FIGURE 7. ○, reflected shock centre, $x_s = u_1 t$; △, reflected shock radius, $r_s = c_1 t$.

the subsequent generation of a nearly cylindrical expansion fan which moves transversely across the shock. In figure 4(*c*) collision of the diffracting shock with the downstream edge of the slit and the generation of a nearly cylindrical reflected shock in a Mach configuration are shown. In figures 4(*d*)–(*f*), spreading of the transverse wave system is evident. The development of an inclined fluid jet emerging from the slit with an accompanying vortex are the main features to be observed in figures 4(*g*)–(*i*). In this case the particle velocity behind the shock is initially subsonic but, since the pressure ratio across the slit is supercritical, choking occurs.

A similar sequence of events is shown in figure 5 (plate 2) for $M_0 = 2{\cdot}14$ and $L = 0{\cdot}953$ cm. In this case the particle velocity behind the undisturbed shock is supersonic, so that a Prandtl–Meyer expansion stands at the upstream edge of the slit and the emerging fluid jet is entirely supersonic. Furthermore, the transverse waves are unable to propagate upstream and remain essentially attached to their point of origin. Outside the slit the reflected shock originating at the downstream edge of the slit is observed to reflect from the jet boundary, giving rise to a complex jet structure.

Figures 4 and 5 clearly demonstrate the attenuation mechanism described

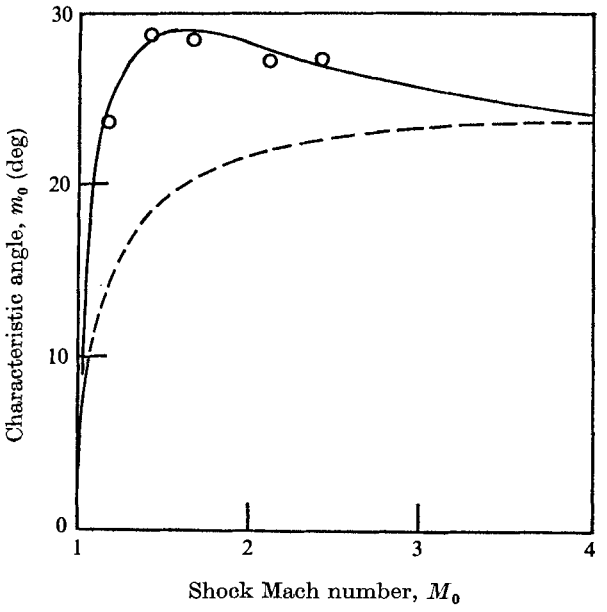

FIGURE 8. Characteristic angle m_0. ○, experiment; ——, acoustic theory, equation (9); – – –, ray-shock theory, equation (2).

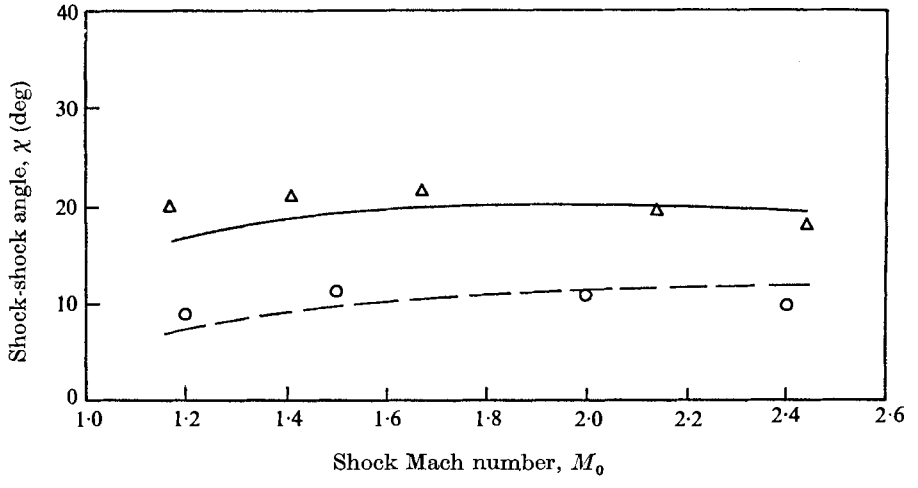

FIGURE 9. Triple point locus angle χ. △, experiment; ——, equation (12); ○, three-shock theory; – – –, ray-shock theory.

earlier as the Mach stem lags behind the incident shock. The attenuated portion of the shock exhibits significant curvature and the Mach stem is normal to the wall only at its foot.

From the photographs various parameters associated with the shock–slit interaction can be measured directly. By a simple geometric construction the radii and centres of the transverse waves may be easily determined. Average wave speeds from each series of photographs are shown in figures 6 and 7. Figure 6

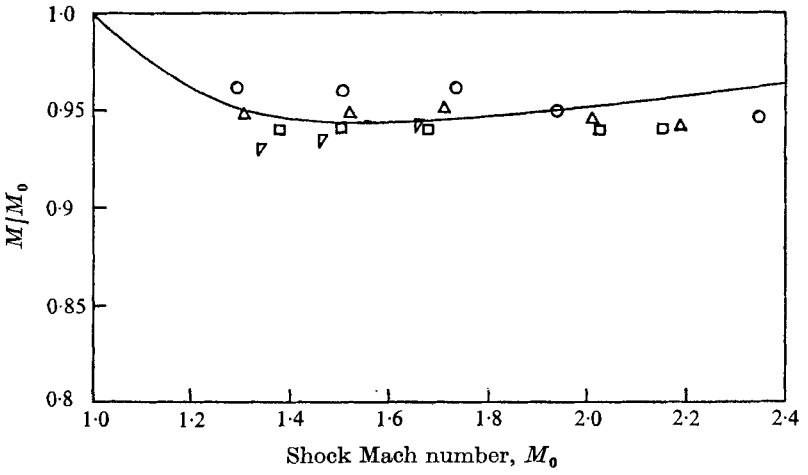

FIGURE 10. Shock wave attenuation. ○, L = 0·173 cm; △, L = 0·635 cm; □, L = 1·905 cm; ▽, L = 3·175 cm; ——, theory, equations (8) and (10).

demonstrates that the expansion wave radius and centre progress uniformly with time and at a rate which is equal to the respective sound speed c_1 and particle velocity u_1 behind the undisturbed shock. With a co-ordinate system located at the downstream edge of the slit, figure 7 shows that the reflected shock spreads out uniformly with an absolute speed that is only slightly lower than the acoustic speed c_1. Interestingly, the shock centre is convected downstream at roughly the same speed as the expansion wave. Thus both transverse waves are initially pseudo-stationary in their respective time frames.

According to the ray-shock theory the locus of the intersection of the head of the expansion wave with the incident shock is linear, the slope being the tangent of the characteristic angle $m(M_0)$. The measured variation in m_0 with shock Mach number is given in figure 8, which may illustrate the rather approximate nature of the ray-shock theory as the predicted values are significantly underestimated, particularly at low shock Mach numbers. The validity of (9) is clearly confirmed by the experimental results, which agree closely with those of Skews (1972).

The triple point locus was also measured from the photographs and observed to be essentially linear. While it is well known that this is correct for simple Mach reflexion, it is not clear why this should be so for the present case, where the incident shock is curved. The photographs do indicate that the degree of shock curvature is small and perhaps this explains the results. From figure 9 it can be seen that the ray-shock theory considerably underestimates the measured values. Similarly, predictions based on a simple straight three-shock configuration are equally inaccurate, which suggests that the error lies in the inability of the theory to account for shock curvature.

Examination of the photographs reveals that, once it has moved well away from the wall, the triple point lies roughly halfway between the break in the Mach stem and the break in the incident shock due to the expansion wave. This suggests the simple empirical relation

$$\chi = \tfrac{1}{2}(\chi' + m_0), \tag{12}$$

where χ' is the value given by the ray-shock theory (or alternatively by the simple three-shock theory) and m_0 is given by (9). Equation (12) is seen to fit the experimental data fairly well except at low shock Mach numbers.

The attenuation of shock-wave velocities can be measured by transducers. The measurements nearly 50 cm downstream of the slit are presented in figure 10 for 4 slit widths ranging from 0·173 to 3·175 cm for an initial shock number M_0 varying from 1·3 to 2·35. It can be seen in figure 10 that the results are predicted reasonably well by (8) and (10) although the theoretical curve does not take into account the additional attenuation due to transverse wave reflexions. Thus the effect of wave reflexions appears to be slight at this point of measurement. As expected, the shock attenuation is quite weak, between 4 and 7 % over the range of the tests. Although the data given in figure 10 correspond to 4 slit widths at various shock Mach numbers, no significant effect of slit widths is discernible. This is in agreement with the ray-shock theory, according to which M and θ are constant along $C+$ characteristics and therefore the same M and θ are good for all slit widths for a given M_0. Physically, the characteristic length (slit width) is absent from the diffraction equations and that process is then self-similar.

As noted earlier, the theoretical solution given here is not strictly correct and it might be supposed that the difficulty lies in the assumption that the Chester function $K(M)$ is constant. Calculations have been carried out using a simpler function developed by Milton (1971) which approximates $K(M)$ fairly closely. However, for $M_0 = 1{\cdot}4$ the results were found not to differ substantially from the solution given above, so it appears that the difficulty lies elsewhere.

Inaccuracies in the ray-shock solution to the Mach reflexion process are evident from Whitham's original paper (1957). Corrections have been recently proposed (Milton 1975) for strong shocks and, although these offer some improvement, calculations have demonstrated that they are still insufficient for the present case where weaker shocks have been considered. Apparently, further modifications of the ray-shock theory to account for the existence of a reflected shock and curvature of the incident shock and Mach stem are required for a more accurate solution of the present problem.

In order to examine the transverse wave reflexion processes more closely, a photographic study was conducted for a channel width of 1·727 cm, a slit width of 0·889 cm and $M_0 = 1{\cdot}4$ with the results shown in figures 11 (*a*)–(*j*) (plate 3). The direction of motion is reversed from that previously shown and the slit is in the lower wall. Owing to inadequate gasket seals some extraneous waves due to leakage are visible in the photographs although these do not appear to compromise seriously the qualitative features of the flow. In figures 11 (*a*) and (*b*) the motion is similar to that shown previously, while in figures 11 (*c*), (*d*) and (*e*) the reflexion of the transverse waves from the upper wall is illustrated, the triple point just arriving at the upper wall in (*e*). It is interesting to note that at this time, which is taken to be the completion of one half-cycle of the motion, the attenuated shock is again nearly plane. Figure 11 (*h*) shows the situation after one complete cycle of the motion as the triple point has just returned to the lower wall. Figure 11 (*j*) shows about one and a half cycles of the motion.

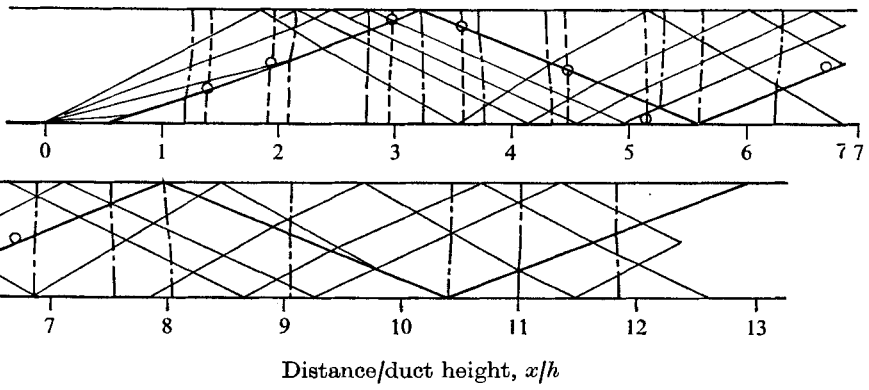

FIGURE 12. Wave diagram showing transverse wave motion on the shock front for $M_0 = 1{\cdot}4$, $L = 0{\cdot}89$ cm, $H = 1{\cdot}73$ cm. O, experimental triple point; ———, shock-shock; – – – –, experimental shock profile; — — —, theoretical shock profile; ———, kinematic wave.

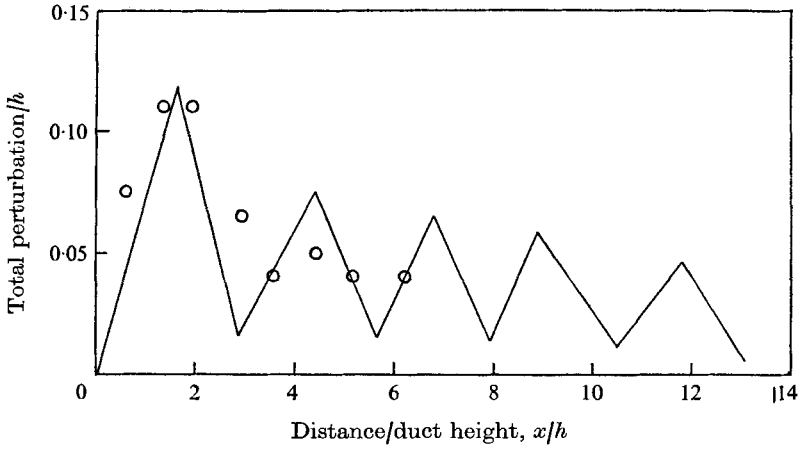

FIGURE 13. Cyclic variation in shock front perturbation for $M_0 = 1{\cdot}4$. ———, wave diagram; O, experiment.

A wave diagram depicting the transverse wave motion on the shock front was constructed for the case corresponding to figure 11 and about two and a half cycles of the theoretical motion are shown in figure 12. The triple point trajectory which represents the Mach reflexion process originating at the downstream edge is shown as a dark heavy line. Clearly, multiple reflexions of the transverse waves lead to increased shock attenuation owing to the wave interactions which are illustrated. As time progresses, the kinematic wave spreads out into the flow field, and the attenuation becomes more continuous and gradual.

The effect of slit width on the attenuation rate can also be deduced from the wave diagram. From the slopes of the characteristics and the shock-shock trajectory it can be seen that increasing the slit width tends to increase the number of transverse wave reflexions, thereby increasing the attenuation rate.

Experimental measurement of the shock-shock trajectory from the schlieren photographs of figure 11 are shown as circles on the wave diagram. The theoretical trajectory is nearly linear and good agreement with experiment is observed over the somewhat limited range of the tests.

From the wave diagram the theoretical shock shape can be traced in with the aid of tabulated results. These are shown as dash–dot lines. It can be seen that the shock curvature varies in a cyclic manner. The experimental shock shape obtained from the photographs is shown on the wave diagram as dashed lines and it can be seen that both the sense and degree of curvature are reasonably well predicted within the scope of the tests.

The wave diagram also demonstrates that the attenuating shock is stable, i.e. perturbations in the wave form tend to decrease as the shock advances down the duct. As shown in figure 13 the wave diagram tends to underestimate the rate at which the shock approaches a planar form. Generally, these results are in accord with those of Lapworth (1959), who examined the stability of shocks perturbed by 'roof-top' obstacles on the side walls of a shock tube.

5. Conclusions

Within its scope, the present investigation has shown that the attenuation of a shock wave by a single transverse slit is relatively weak, only about 7 % for the largest slit width tested. The gradual nature of the attenuation process is controlled by transverse wave motion which is initially pseudo-stationary, so that the initial attenuation is independent of slit width in accordance with the ray-shock theory. The presence of a back wall eventually destroys this self-similar motion and leads to a weak additional attenuation of the travelling shock.

Increasing the slit width produces only a relatively small increase in attenuation rate some distance downstream of the slit, therefore the most efficient immediate attenuation would be produced by a series of closely spaced narrow slits.

A wave diagram constructed according to the ray-shock theory faithfully describes the transverse wave motion over roughly the first two cycles of the motion, provided that an empirical relation for the triple point locus angle is employed. Stability of the attenuating shock is clearly demonstrated by the wave diagram technique.

This work was supported by the National Research Council of Canada under Grant no. A-1255. The authors wish to thank P. Lee, O. Muehling, R. Neemeh and N. Elabdin for their assistance.

REFERENCES

LAPWORTH, K. C. 1959 An experimental investigation of the stability of plane shock waves. *J. Fluid Mech.* **6**, 469.

MILTON, B. E. 1971 Shock wave motion and focusing in area contractions. Ph.D. thesis, University of New South Wales, Australia.

MILTON, B. E. 1975 Mach reflection using ray-shock theory. *A.I.A.A. J.* **13**, 1531.

OSHIMA, K., SUGAYA, K., YAMAMOTO, M. & TOTOKI, T. 1965 Diffraction of a plane shock around a corner. *Inst. Space Aero. Sci., Univ. Tokyo, Rep.* no. 393.

SKEWS, B. W. 1972 The shape of a shock wave in regular reflection from a wedge. *Can. Aero. & Space Inst. Trans.* **5**, 28.

WHITHAM, G. B. 1957 A new approach to problems of shock wave dynamics. Part 1. Two-dimensional problems. *J. Fluid Mech.* **2**, 145.

WHITHAM, G. B. 1958 On the propagation of shock waves through regions of non-uniform area or flow. *J. Fluid Mech.* **4**, 337.

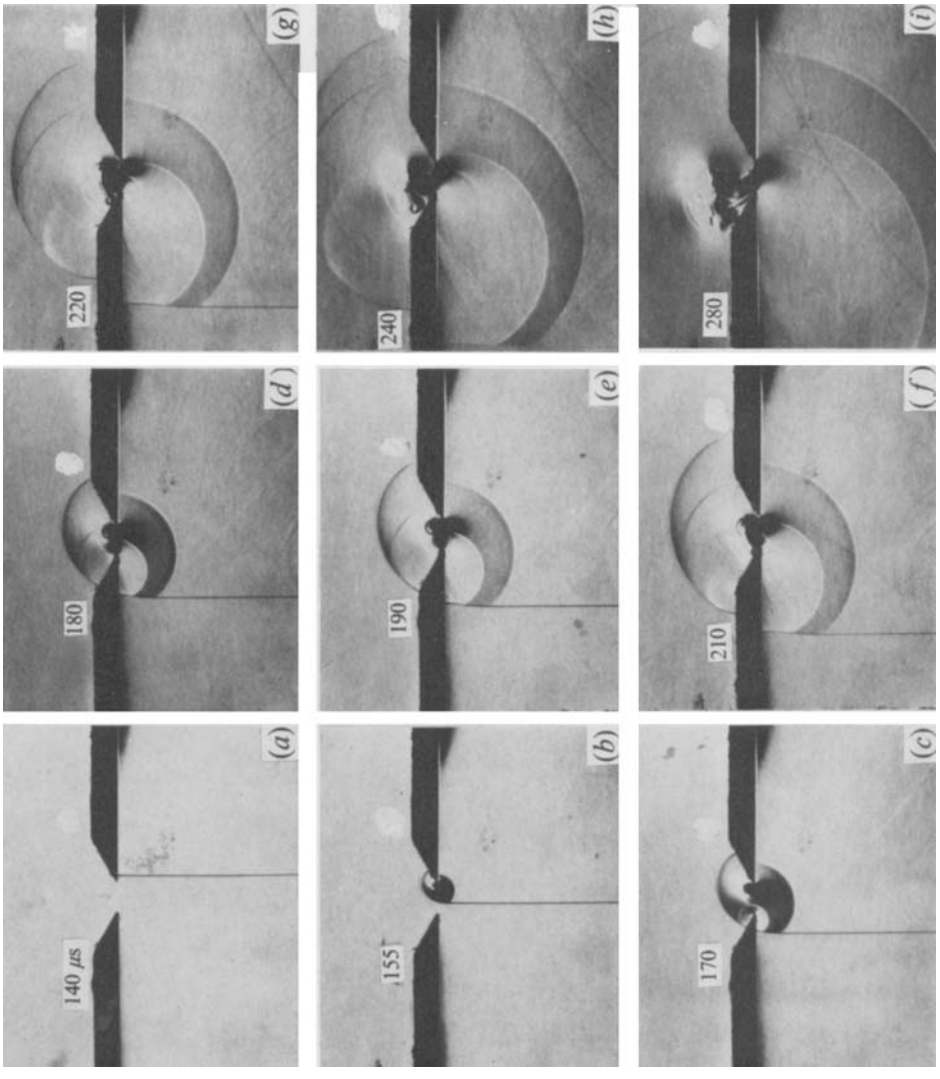

FIGURE 4. Shock–slit interaction for $M_0 = 1{\cdot}4$, $L = 0{\cdot}699$ cm.

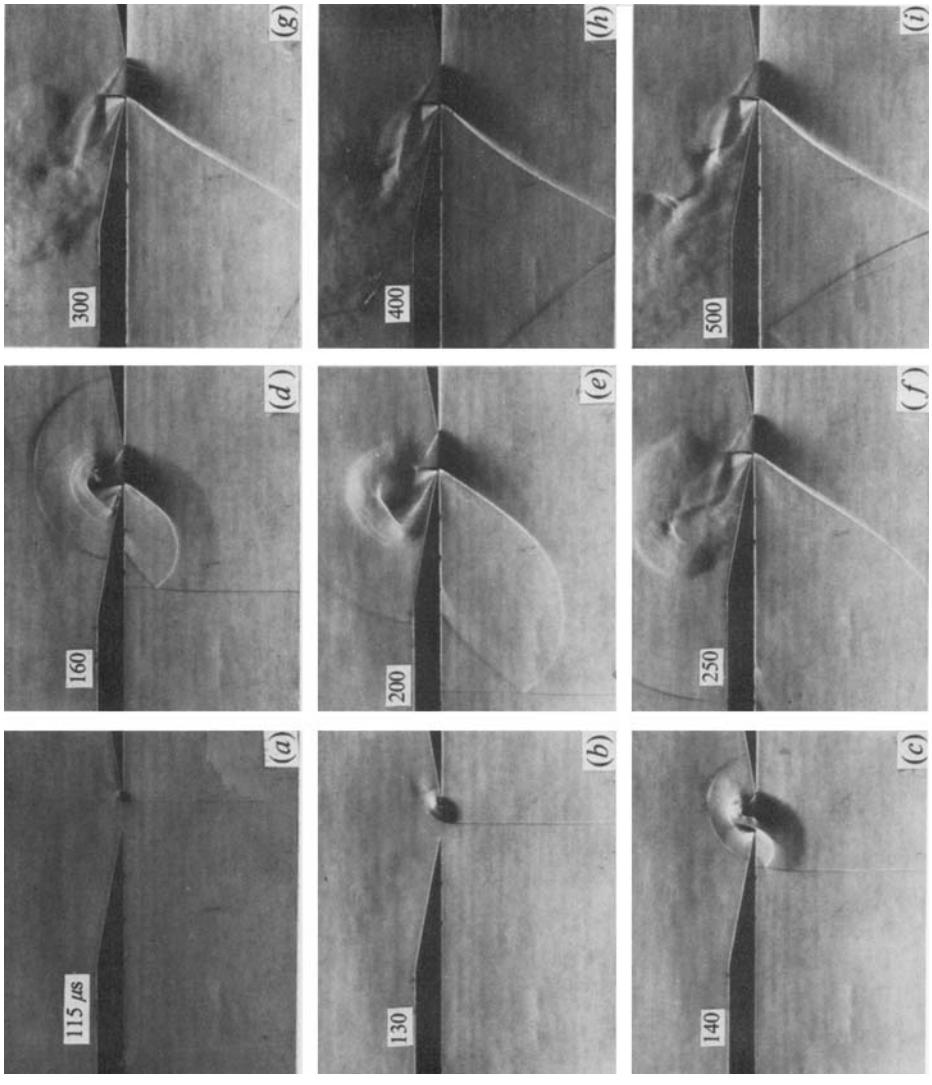

FIGURE 5. Shock–slit interaction for $M_0 = 2{\cdot}14$, $L = 0{\cdot}953$ cm.

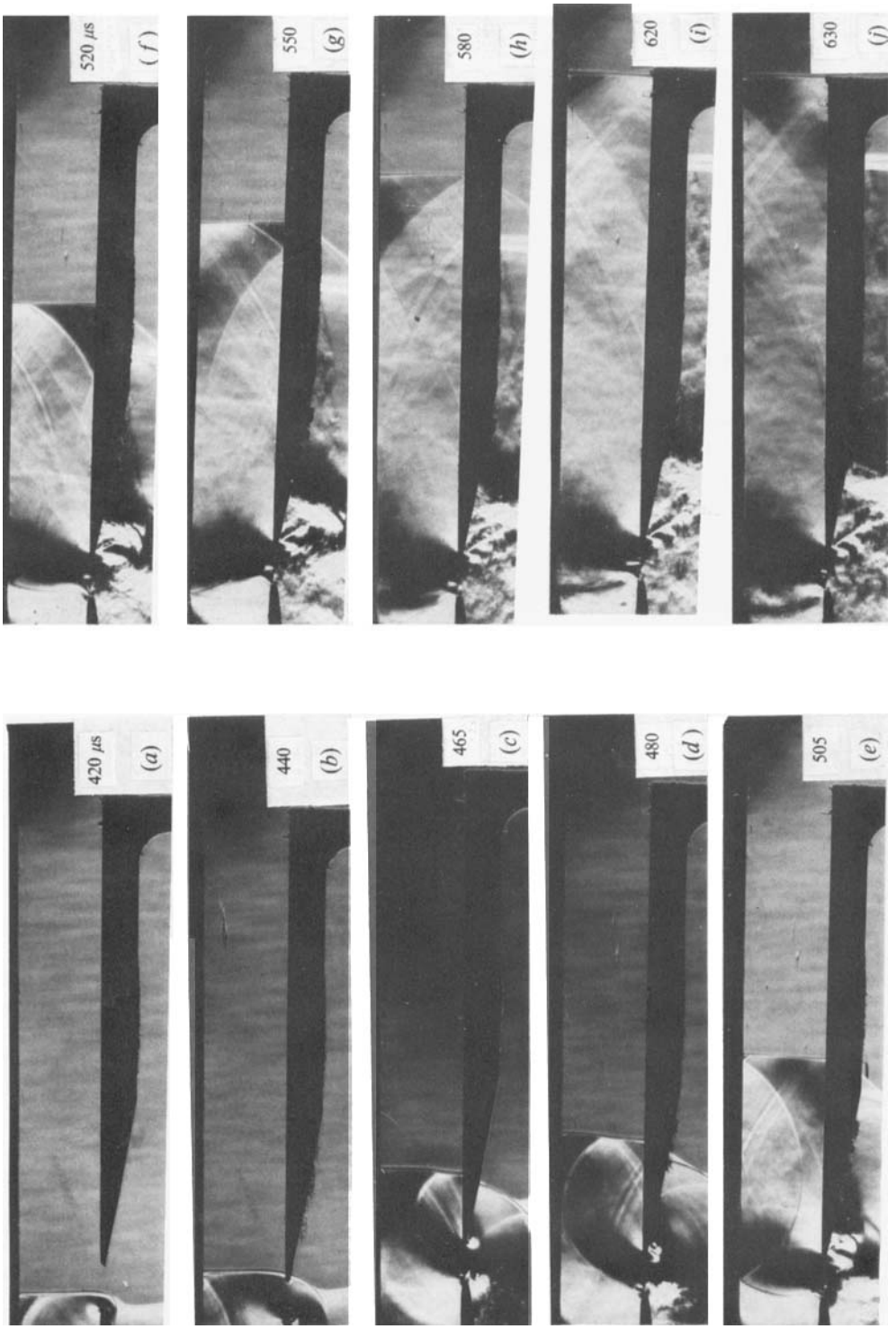

FIGURE 11. Shock–slit interaction for $M_0 = 1{\cdot}4$, $L = 0{\cdot}89$ cm.